

Deposition and Removal of Fugitive Dust in the Arid Southwestern United States: Measurements and Model Results

Vic Etyemezian, Sean Ahonen, and Djordje Nikolic

Division of Atmospheric Sciences, Desert Research Institute, Las Vegas, Nevada

John Gillies and Hampden Kuhns

Division of Atmospheric Sciences, Desert Research Institute, Reno, Nevada

Dale Gillette

Air Resources Laboratory (MD-81), Applied Modeling Research Branch, Research Triangle Park, North Carolina

John Veranth

Department of Pharmacology and Toxicology, University of Utah, Salt Lake City, Utah

ABSTRACT

This work was motivated by the need to better reconcile emission factors for fugitive dust with the amount of geologic material found on ambient filter samples. The deposition of particulate matter with aerodynamic diameter less than or equal to $10\ \mu\text{m}$ (PM_{10}), generated by travel over an unpaved road, over the first 100 m of transport downwind of the road was examined at Ft. Bliss, near El Paso, TX. The field conditions, typical for warm days in the arid southwestern United States, represented sparsely vegetated terrain under neutral to unstable atmospheric conditions. Emission fluxes of PM_{10} dust were obtained from towers downwind of the unpaved road at 7, 50, and 100 m. The horizontal flux measurements at the 7 m and 100 m towers indicated that PM_{10} deposition to the vegetation and ground was too small to measure. The data indicated, with 95% confidence, that the loss of PM_{10} between the source of emission at the unpaved

road, represented by the 7 m tower, and a point 100 m downwind was less than 9.5%. A Gaussian model was used to simulate the plume. Values of the vertical standard deviation σ_z and the deposition velocity V_d were similar to the U.S. Environmental Protection Agency (EPA) ISC3 model. For the field conditions, the model predicted that removal of PM_{10} unpaved road dust by deposition over the distance between the point of emission and 100 m downwind would be less than 5%. However, the model results also indicated that particles larger than $10\ \mu\text{m}$ (aerodynamic diameter) would deposit more appreciably. The model was consistent with changes observed in size distributions between 7 m and 100 m downwind, which were measured with optical particle counters. The Gaussian model predictions were also compared with another study conducted over rough terrain and stable atmospheric conditions. Under such conditions, measured PM_{10} removal rates over 95 m of downwind transport were reported to be between 86% and 89%, whereas the Gaussian model predicted only a 30% removal. One explanation for the large discrepancy between measurements and model results was the possibility that under the conditions of the study, the dust plume was comparable in vertical extent to the roughness elements, thereby violating one of the model assumptions. Results of the field study reported here and the previous work over rough terrain bound the extent of particle deposition expected to occur under most unpaved road emission scenarios.

IMPLICATIONS

This work was motivated by the well-documented disagreement between estimates of road and other geological dust obtained by emissions inventory methods and the actual amount of inorganic minerals observed on filter samples at ambient monitoring sites. This study provides a basis for modeling the magnitude of PM_{10} dust removal by deposition close to the emission source. The analysis focuses on emissions from unpaved roads, though the results may be pertinent to other sources of fugitive dust.

INTRODUCTION

Fugitive dust is emitted from an unpaved road when a vehicle passes and disturbs the surface, raising a cloud of dust that begins to travel downwind. Initially, the cloud is dense; with travel downwind, the cloud is dispersed by turbulent eddies in the atmosphere. Particles suspended in the cloud can be removed by gravitational settling, by interaction with the ground surface, terrain anomalies (e.g., buildings, boulders, etc.), or vegetative cover in the downwind fetch of the unpaved road.

Watson and Chow¹ documented the discrepancy between emission inventories for particulate matter with aerodynamic diameter less than or equal to $10\ \mu\text{m}$ (PM_{10}) fugitive dust and the source attribution of ambient filter samples. Their analysis indicated that the amount of geologically derived PM_{10} found in the air is smaller than would be expected based on emission inventories and dispersion models. Countess² summarized 11 shortcomings in the current treatment of fugitive dust emissions. One of the recommendations made by Countess² was to upgrade existing models with “sub-models” to account for the removal of particles near the source. Based on the analysis of PM_{10} concentrations downwind of an unpaved road, Watson and Chow¹ hypothesized that coarse particles in the PM_{10} range deposit rapidly within the first several hundred meters downwind of the road. That analysis did not consider the vertical dispersion of PM with

distance downwind, resulting in a great overestimate of the effect of near-source deposition.

In this paper, the results of the Ft. Bliss measurements of the near-source removal of PM_{10} dust emitted from an unpaved road are presented and compared with predictions from a simple dispersion model. These data provide an estimate of the fraction of PM_{10} fugitive dust emissions from unpaved roads that is regionally transportable. Results of the Ft. Bliss study are also compared with the earlier measurements of Veranth et al.,³ which were obtained under significantly different terrain and atmospheric stability conditions.

BACKGROUND

Figure 1 schematically illustrates the progression of a dust plume emitted behind a vehicle and advected downwind over a vegetative cover. In the region (A) where the dust cloud first meets the vegetation, dust particles may be removed by individual vegetation elements. Some work in the area of particle removal by windbreaks may be applicable to this “impact zone,”⁴ although the specific formulation would have to be adjusted for vegetative covers with a long fetch (as opposed to a windbreak that is only several meters deep).

Very far downwind (region C in the figure), the dust plume approaches a steady vertical concentration profile that is nearly invariant with transport distance. In

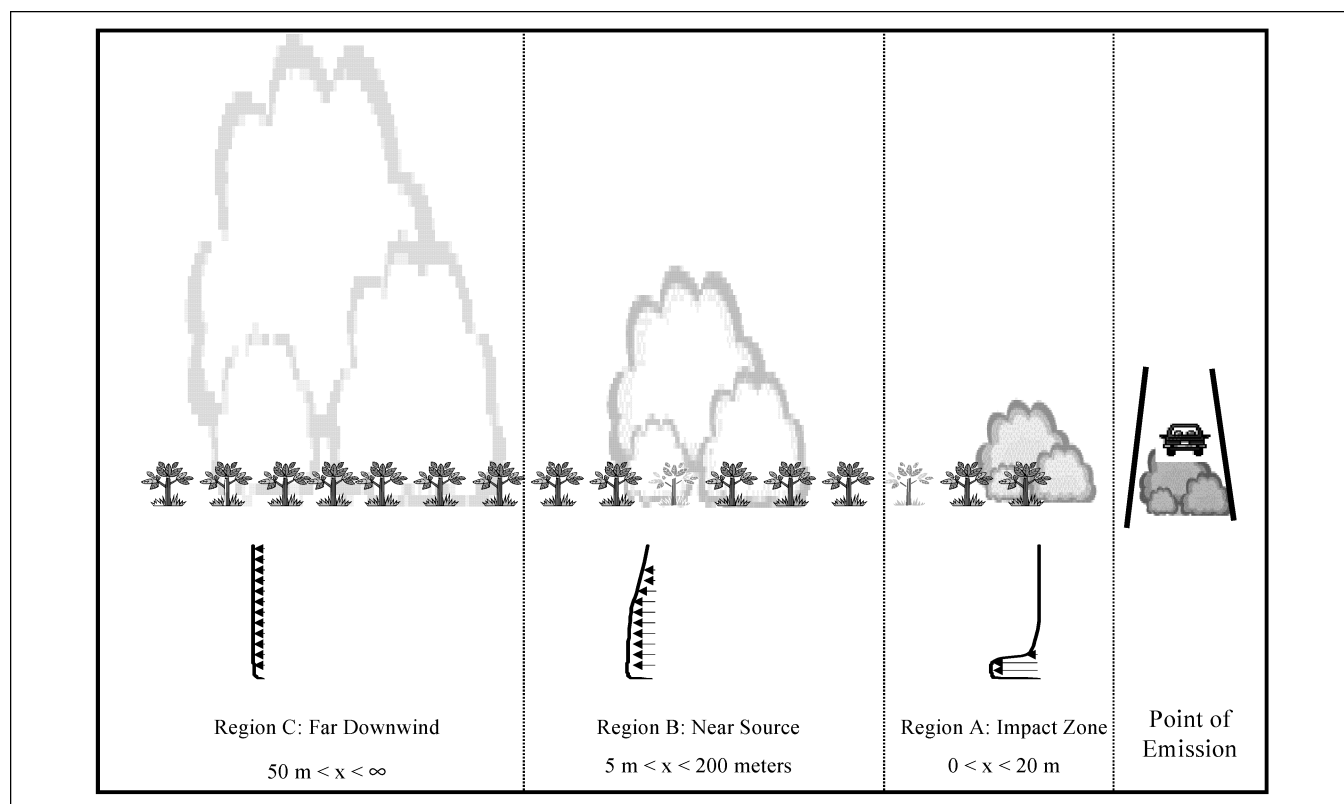


Figure 1. Development of a dust plume downwind of an unpaved road.

between the “impact zone” and “far downwind” lies the “near-source” region, where the concentration profile of dust particles is changing with transport distance; specifically, the dust plume is expanding in the vertical direction.

Whereas deposition serves to permanently remove particles from the airstream, turbulent dispersion causes particles to dynamically redistribute through the mixed layer in the atmosphere. Dispersion causes pockets of air with comparatively high concentrations of particles to be diluted with pockets of air that have lower concentrations.

Vertical dispersion is commonly quantified as a dispersion coefficient multiplied by a concentration gradient. The amount of particles crossing a horizontal plane is given by an equation of the following form:

$$F_z(z) = -K_{zz}(z) \frac{\partial C}{\partial z} \quad (1)$$

where F_z (g/m²/s) is the vertical flux of particles at a height z and is equal to the vertical (z -direction) dispersion coefficient K_{zz} (m²/s) multiplied by the negative of the vertical concentration gradient (g/m⁴). Similar equations are used to describe dispersion in the two horizontal directions with the coefficients K_{xx} and K_{yy} , which may be close in magnitude to one another but can be quite different from K_{zz} . Dispersion parallel to the road may be ignored if the source is continuous in time and approximated by an infinitely long line (e.g., a long road).

In the surface layer (nominally <50 m above ground), where the flux of momentum to the ground is constant with height, K_{zz} can be directly measured with meteorological instrumentation. At greater heights, measurements are more difficult, and the functional form of K_{zz} is inferred from wind tunnel tests, theory, or numerical simulations.^{5–7}

An alternative method for modeling diffusion is to specify the physical degree of the spread of a plume as a function of downwind distance and atmospheric stability. This is the approach used by a number of Gaussian plume models, including the ISC3.⁸ The concentration of an airborne species is assumed to be normally distributed in each of the three ordinal directions, with standard deviations of σ_x , σ_y , and σ_z . For a continuous line source, dispersion in the horizontal plane can be ignored. The parameter σ_z has been specified by a number of authors including Gifford,⁹ Klug,¹⁰ Turner,¹¹ and Martin.¹² The ISC3 model uses the formulation of Turner.¹¹ The Gaussian approach is useful because of its simplicity in implementation. However, it has its limitations, most notably, that the assumption of a normally distributed

concentration profile may be too simple to adequately account for the range of land use and atmospheric conditions that can be encountered.

Alternative methods for quantifying turbulent dispersion are available from the literature,^{7,13,14} some of which may be more accurate than the simple mixing-length or Gaussian models. Venkatram⁷ argues that eq 1 is flawed because it does not account for changes in air density with height. That is, eq 1 does not reflect the fact that the requirement of zero net flux in the vertical direction can be satisfied physically by a constant mixing ratio, even if there exists a concentration gradient in the vertical direction. Du and Venkatram¹³ propose a method to specify the vertical dispersion based on the friction velocity u_* and the Monin–Obukhov length L , rather than strictly from the stability class. Schopflocker and Sullivan¹⁴ encourage the use of two probability density functions (pdf) to specify the vertical distribution of concentration instead of a single pdf, as is done in Gaussian plume formulations. These authors suggest that two pdfs are required to represent both the high-level concentration distributions in the “thin sheets” that are formed in turbulent diffusion as well as the distribution of low-level concentrations found outside the sheets.

Dry deposition of particles is frequently modeled analogous to resistance in an electrical circuit.^{4,15–17} Most of the models developed to study dry deposition of sulfate and other pollutants from the atmosphere are derived for the well-mixed conditions of region C in Figure 1. The flux to the ground is assumed to be equal to the concentration measured at a given height multiplied by a transfer coefficient, which is also dependent on height. The transfer coefficient is called the deposition velocity and is given by the symbol V_d (m/sec). Thus, according to the resistance model

$$F_{\text{dep}} = C(z) V_d(z) \quad (2)$$

where F_{dep} is the vertical flux of material to the ground (g/m²/s) and $C(z)$ is the height-dependent concentration. The deposition velocity is given as the inverse of three resistances in series, that is:

$$v_d(z) = \frac{1}{r_a(z) + r_b + r_c} \quad (3)$$

where r_a is the resistance to aerodynamic transport through the surface layer and is dependent on the height z above the surface; r_b is the resistance to transport through the “quasi-laminar sublayer,” and r_c is the resistance to collection on the surface or vegetative elements (the subscripts a, b, and c are unrelated to the regions in

Figure 1). This model for deposition is built on the assumption that close to the ground, that is, from the top of the surface layer down, the flux of a depositing species is constant with height. Related to the assumption of constant flux, the model also assumes that the concentration profile through the surface and quasi-laminar layers is not changing significantly over time. This corresponds strictly only to region C in Figure 1, though it may also hold approximately for region B.

In addition to turbulent transport through the surface and quasi-laminar layers, particles are also influenced by gravity. This effect can be embodied in the resistance model by assuming that gravitational settling represents another resistor (r_g) acting in parallel with those in eq 3. Using the more familiar settling velocity v_g ($= 1/r_g$), which is a well-known function of the particle size,¹⁸ the deposition velocity can be expressed as

$$v_d(z) = \frac{1}{r_a(z) + r_b + r_a(z)r_b v_g} + v_g. \quad (4)$$

Note that in arriving at eq 4, we have assumed that the surface resistance to deposition, r_c , is very small for particles in the size range of interest (aerodynamic diameters less than 10 μm). That is, once a particle impacts on a collector, it sticks to that collector and is permanently removed from the atmosphere. Deviations from this ideal are not considered here, but are addressed by others.^{15,19,20} For stable and unstable atmospheric conditions, the aerodynamic resistance r_a is given by the U.S. Environmental Protection Agency (EPA)⁸ based on the work of Byun and Dennis.²¹ r_a is dependent on the friction velocity u_* , the roughness length z_0 , the Monin–Obukhov length scale L , and a reference z_r . The quasi-laminar resistance r_b is a function of the particle Schmidt number, Stokes number, and the flow friction velocity (u_*).^{8,22} The Schmidt number accounts for Brownian motion whereas the Stokes number accounts for inertial impaction, which is the usually dominant pathway for deposition of particles with diameters of 1–10 μm . This model for dry deposition requires that the airflow parameters u_* , z_0 , and L are known.

METHODS

Field Measurements

From April 11 through April 24, 2002, field experiments were performed at an unpaved road on the open range of Ft. Bliss, a military facility near El Paso, TX. The experimental procedure was based on an upwind/downwind technique that has been used by other investigators (e.g., Gillies et al.²³ and Cowherd²⁴). Three towers were set up collinearly and perpendicular to a 1000-m section of

unpaved road (Figure 2), which was oriented in a north–south direction. Historical meteorological data indicated that winds at this time of year were predominantly from the west. Brief rain occurred during the study period but the soil surface dried rapidly due to springtime wind and sun. During all tests reported here, the unpaved road was dry and the soil moisture content for at least the top several centimeters was near zero.

Tower 1, at 7 m downwind, had measurement positions spaced logarithmically at 0.76, 1.28, 2.66, and 5.17 m above ground level (AGL). Tower 2, at 50 m downwind, had measurement positions at 1.25, 2.6, 5.7, and 12.2 m AGL. Tower 3, at 100 m downwind, had the same measurement positions as Tower 2, with an additional sampling location at 0.4 m AGL. One hundred meters was chosen as the maximum practical downwind distance for placing the furthest tower. This was to ensure that the dust plume originating at the unpaved road, which expands in the vertical direction as it advects horizontally, would be mostly contained within the height of the 12.2-m tall tower. Four anemometers, one wind vane, and one temperature probe were mounted on Tower 3 to characterize the local meteorological conditions. PM_{10} dust concentrations were measured simultaneously at all of the tower measurement positions with DustTrak monitors (Model 8520, TSI, Inc., Shoreview, MN). The DustTrak is a rugged portable instrument that uses particle light scattering to infer PM concentrations. The DustTrak was chosen because it operates over a wide range of particle concentrations spanning 0.001–100 mg/m^3 and provides the fast-response measurements (1 Hz) needed to detect individual road dust plumes. The flow rate at the instrument inlet is 1.7 lpm; for the data presented here, the instrument has been equipped with a nominal PM_{10} inlet provided by the manufacturer. The instrument is calibrated by the manufacturer with the respirable fraction of an Arizona Road Dust standard (ISO 12103–1, A1) to relate light scattering intensity at 90° with respect to the incident laser light to aerosol mass concentrations in mg/m^3 . The ISO 12103–1, A1 standard consists of primarily silica particles (>70%) that are provided with some particle size specifications. By volume, the standard consists of 1–3% particles with diameters less than 1 μm , 36–44% with diameters less than 4 μm , 83–88% with diameters less than 7 μm , and 97–100% with diameters less than 10 μm .

Niu et al.²⁵ found that in comparing data from four DustTraks collocated in an indoor environment, the interinstrument variability was a reasonable 3%. Several authors have also reported that DustTrak measurements correlate well with filter-based measurements of diesel exhaust,²⁶ ambient urban particulate matter,²⁷ and indoor airborne particles,²⁵ though in all cases, investigators

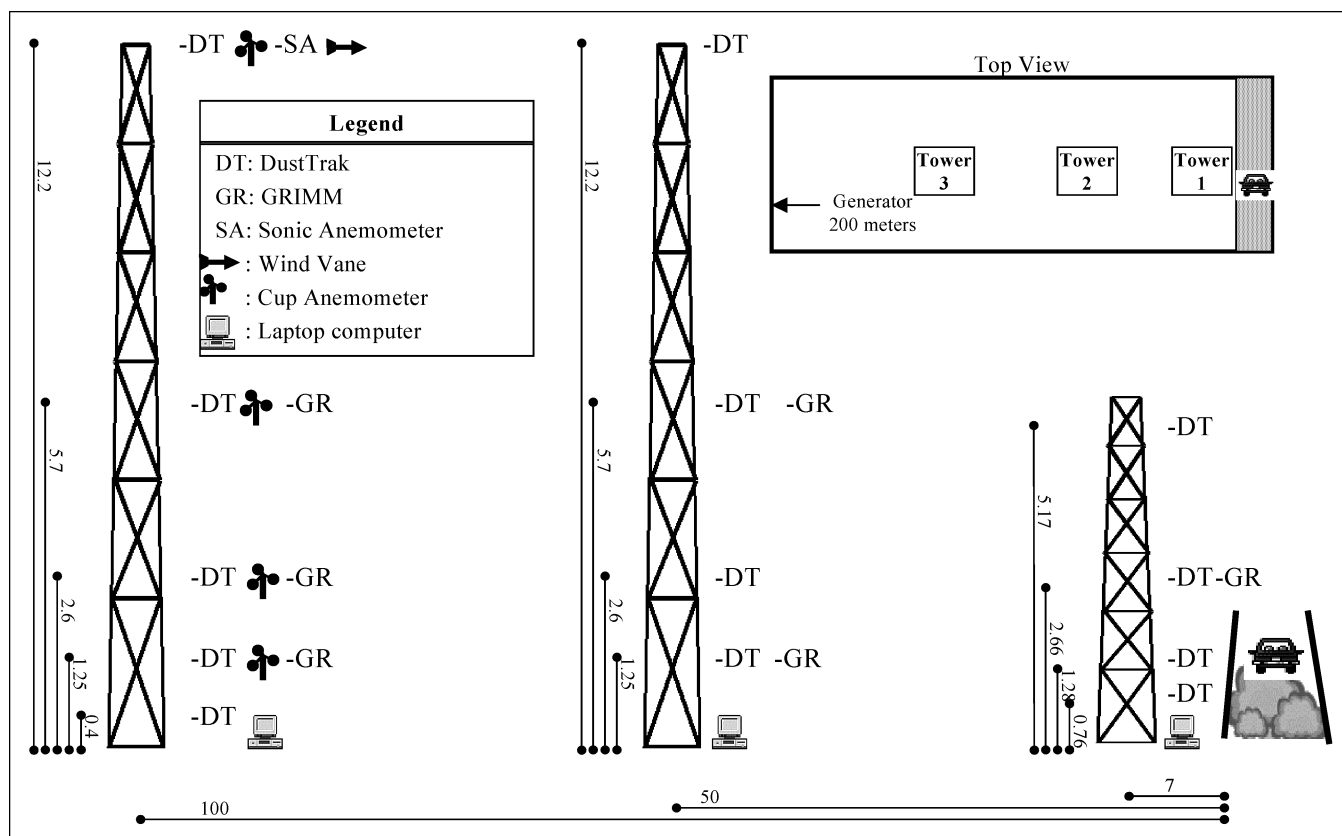


Figure 2. Schematic of equipment setup at Ft. Bliss during the April 2002 field campaign. The vertical and horizontal components are drawn on different scales. Dimensions are in meters.

noted that the DustTrak deviated from filter-based measurements by a factor that depends on the nature of the aerosol measured. One shortcoming of using a nephelometer-style instrument is that light scattering response to changes in mass concentration can depend strongly on particle composition as well as particle size. Based on manufacturer specifications for the DustTrak, the greatest change in light scattering per unit mass for silica aerosols occurs for particles with a diameter of around $0.4 \mu\text{m}$. The instrument is less sensitive to changes in mass concentration of smaller or larger particles. For $10\text{-}\mu\text{m}$ particles, light scattering sensitivity to changes in mass concentration is approximately a factor of 50 less than for $0.4\text{-}\mu\text{m}$ particles. This suggests that two different values measured by the DustTrak may not necessarily translate into proportional differences in actual PM_{10} mass concentration, especially if the two measurements represent airborne particles that are either substantially different in composition or in particle size distribution. We note that this potential source of uncertainty should not be of great concern for the results presented in this study because the DustTraks are used to provide only a relative measure of PM_{10} flux between the three towers downwind of the unpaved road, the composition of the aerosol measured by all instruments used is constant, and the particle size distribution does not change appreciably over the

distance spanned by the three towers (see Results and Discussion).

During the course of the study, four GRIMM model 1.108 particle size analyzers (GRIMM Tech. Inc., Atlanta, GA) were deployed at various locations and different measurement periods to provide information on the particle size characteristics of the emitted dust. The GRIMM 1.108 is an optical particle counter with 15 particle size bins that cover the range of particles with diameters between $0.3 \mu\text{m}$ and $20 \mu\text{m}$. To estimate aerodynamic particle diameters from the "optical" diameters measured by the GRIMM, we invoke the assumption of spherical particles and the approximation that the density of all particles is equal to that of silica with the following formula:

$$D_j^{\text{aero}} = D_j^{\text{opt}} \sqrt{\rho_p C_c (D_j^{\text{opt}})} \quad (5)$$

where D_j^{aero} is the estimated representative aerodynamic diameter for bin j , ρ_p is the specific density of particles (2.6 for silica), C_c is the Cunningham slip correction factor, and D_j^{opt} is the geometric mean of the minimum and maximum "optical" diameter associated with bin j and given by the formula

$$D_j^{\text{opt}} = \exp \left[\frac{\ln(D_j^{\text{min}}) + \ln(D_j^{\text{max}})}{2} \right] \quad (6)$$

where D_j^{\min} and D_j^{\max} are the nominal smallest and largest diameters in bin j according to the manufacturer of the instrument.

The data stream from the DustTraks, GRIMMs, and meteorological instruments were collected in 1-s intervals on a PC located at the base of each tower. Analysis of the DustTrak data indicated that baseline drift over the course of a day, generally less than $50 \mu\text{g}/\text{m}^3$, did not affect all instruments equally. Thus, a baseline for each instrument was calculated approximately every 20 min over the course of the day from background concentrations measured during periods when there were no dust emissions from the unpaved road.

PM_{10} emissions were created by having a number of test vehicles travel back and forth along the test section of the road. The test vehicles traveled at set speeds of 16, 24, 32, 40, 48, 56, 64, 72, and 81 km/hr. Not all vehicles attained the highest speeds for safety considerations. After two passes (one heading south and one returning north) at the same speed, the vehicle speed was increased incrementally to the highest attainable value and then decreased incrementally to the minimum value. This cycle was then repeated as time allowed. Test vehicles paused for approximately $1 \frac{1}{2}$ min between passes to allow for the dust plume to clear all three downwind towers.

PM_{10} emissions fluxes were calculated for each downwind tower according to the assumption that each DustTrak represented the PM_{10} concentration over a prescribed height interval. The first monitor was assumed to represent the concentration from the ground surface to midway between the first and second monitors. The highest monitors represented the concentrations from midway between the top two monitors to 6.63-m AGL at Tower 1 and 16.06-m AGL on Towers 2 and 3. Intermediate monitors represented the interval spanned by the midpoints to the adjacent monitors. The time series of PM_{10} concentrations were examined for each instrument. Every peak in concentration was associated with an individual vehicle pass, and each pass was visually assigned a start and stop time. Figure 3 shows an example of a concentration time series and the determination of peak start and stop times. The emission flux of PM_{10} from every vehicle pass for each downwind tower was calculated with the sum of the 1-s PM_{10} fluxes with the following equation:

$$EF = \sum_{\text{startofpeak}}^{\text{endofpeak}} \left\{ \cos(\theta) \sum_{i=1}^4 u_i C_i \Delta z_i \Delta t \right\} \quad (7)$$

where EF is the emission flux of PM_{10} in grams per kilometer, θ is the angle (1-s measurement) between the wind

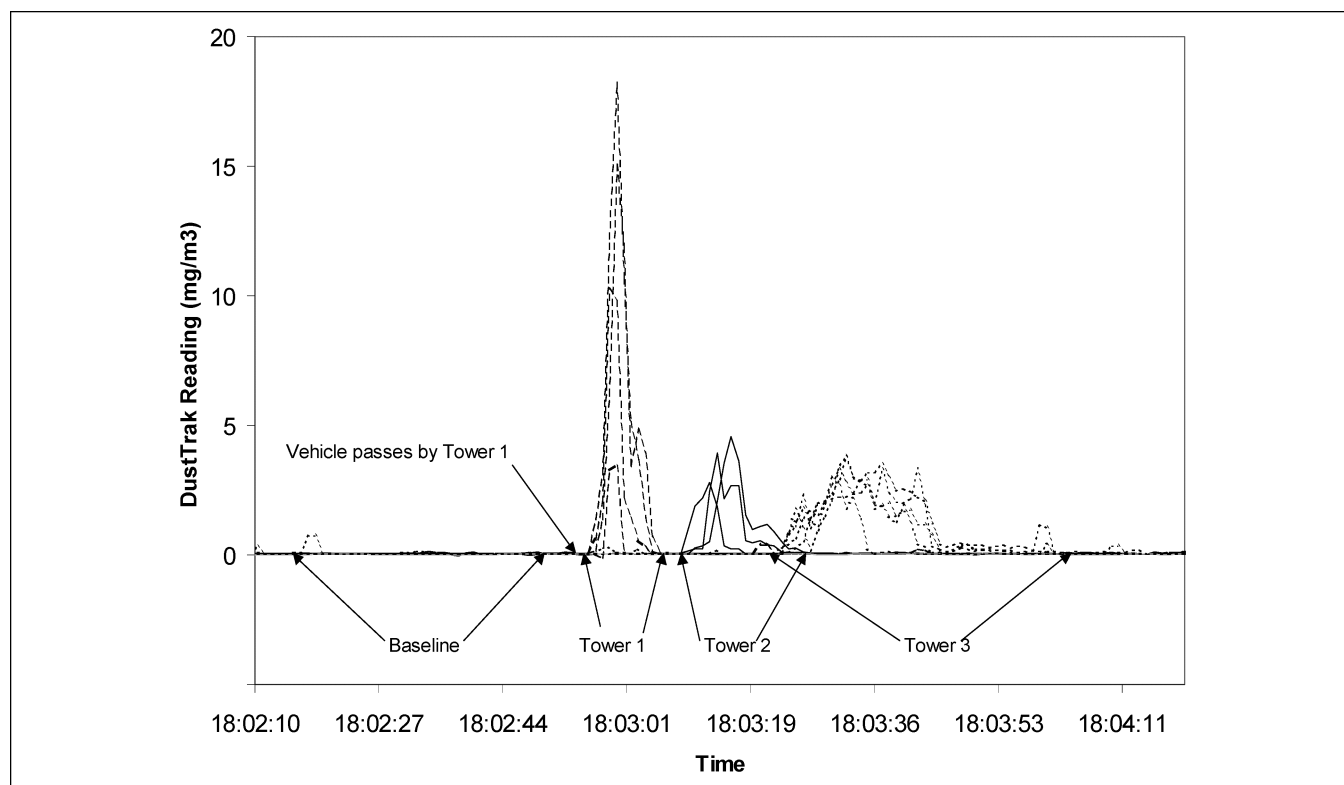


Figure 3. Example of time series of DustTrak PM_{10} concentrations after the passage of a vehicle on the unpaved road at Ft. Bliss. The arrows in the figure illustrate the start and stop times estimated for a baseline reading and the dust plume passing through the downwind Towers 1, 2, and 3.

direction and a line perpendicular to the road, i is one of the four positions (five for Tower 3) of the monitors on the tower, u_i is the average wind speed in m/sec over the interval represented by the i^{th} monitor, C_i is the baseline-corrected PM_{10} concentration in mg/m^3 as measured by the i^{th} monitor over the period Δt , Δz in m is the vertical interval represented by the i^{th} monitor, Δt is 1 s.

The unpaved road at Ft. Bliss was 1 km in length and oriented in the north-south direction, with the three towers lined perpendicular to and east of the road. Even though the angle between the wind vector and the road was accounted for by the $\cos(\theta)$ term in eq 7, when winds did not have a strong westerly component, the dust plume generated by passing vehicles did not travel in the direction of the towers. Only when the 30-s, vector-averaged wind direction fell in the quadrant spanned by the northwest and southwest vectors was the corresponding vehicle pass considered valid. The averaging time was chosen to be 30 s because this is roughly how long it takes the plume to travel from the unpaved road to the 100 m downwind tower. When applying eq 7, 1-s values of wind direction were used.

The wind speed and direction were measured only at the far downwind tower (Tower 3). Therefore, to use eq 7, it was necessary to use wind speeds and directions measured at Tower 3 for Tower 1 and Tower 2. The possibility of introducing errors by this method was examined. The horizontal PM_{10} fluxes were calculated for Tower 3 only and averaged over the test vehicle speed. This procedure was performed twice—once with wind data that corresponded to the time of the passing of the dust plume and once with wind data that was retarded by 30 s. For example, the flux at 13:30:00 was calculated with wind data measured at 13:30:00 and also with wind data measured at 13:29:30. The purpose of this exercise was to subject the flux calculations for Tower 3 to the same uncertainties that the data from Tower 1 and Tower 2 would be experiencing. In comparing the two resulting sets of horizontal fluxes, no significant differences were found (slope = 1.01, $R^2 = 0.98$, $n = 53$, intercept was forced to 0), indicating that the use of Tower 3 wind direction and wind speed to calculate horizontal fluxes of PM_{10} at Tower 1 and Tower 2 would not introduce biases.

The friction velocity and aerodynamic roughness length (u_* and z_0 , respectively) were estimated by assuming that the wind profile was logarithmic:

$$u(z) = \frac{u_*}{\kappa} \ln\left(\frac{z}{z_0}\right) \quad (8)$$

where κ is the von Karman constant and equals 0.4. To obtain meaningful estimates of the bulk quantities u_* and

z_0 , data were averaged over 15-min intervals to obtain the vertical distribution of wind speeds. The final value of 0.005 m obtained for z_0 lies between those expected for “level desert” (0.001 m) and “lawn” (0.01 m).¹⁸ Figure 4 shows the distribution of u_* values that occurred over the course of the field study. Ninety-five percent of the values of u_* fell between 10 and 50 cm/sec, with values between 30 and 40 cm/sec occurring most frequently (35%).

The experiments at Ft. Bliss examined the downwind plume from a vehicle that traversed an unpaved road. The time series of the concentration measured at the downwind towers reflects the influence of a moving point source (see Figure 3). To compare the Ft. Bliss data with the continuous line source models, the concentration time series was integrated for each vehicle pass and each location on the tower, that is:

$$C_{\text{int},k} = \int_{\text{peakstart}}^{\text{peakend}} C_k dt \quad (9)$$

where $C_{\text{int},k}$ is the integral of the concentration C_k at tower location k . Although the location of the particle monitoring instruments (DustTraks) varied slightly from one tower to the next, all towers were equipped with one monitor at a height of 1.26 m. Thus, the integrated concentrations for each individual pass and at each height on a tower were normalized by the integrated concentration at 1.26 m for that tower. The concentration profile from each of 116 passes was placed in a category according to the value of the friction velocity, u_* , associated with that pass. The normalized concentration profiles were then averaged within each friction velocity category. There were four categories in all for u_* , corresponding to bins centered at 0.2, 0.3, 0.4, and 0.5 m/sec. For example, all concentration profiles with a u_* between 0.15 and

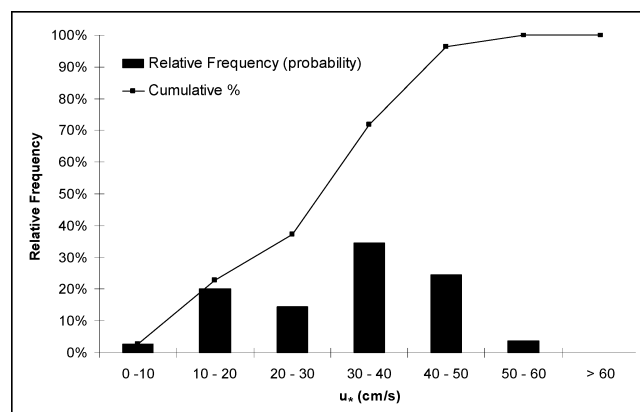


Figure 4. Frequency distribution and cumulative distribution of friction velocity u_* for the 116 15-min intervals corresponding to periods when testing was ongoing at Ft. Bliss. Values are based on a roughness length, z_0 , equal to 0.005 m.

0.25 m/sec were lumped together under the category $u_* = 0.2$ m/sec.

The data from the described fieldwork were collected under neutral to unstable atmospheric conditions in a sparsely vegetated desert with sand dunes 0.1–0.3 m high on generally level terrain. For comparison, a similar data set was collected by Veranth et al.³ under a stable atmosphere and over a substantially rougher terrain. A brief description of that work is given below, and the reader is referred to the original article³ for further details. The fieldwork was conducted in collaboration with the Mock Urban Setting Test (MUST) at the Dugway Proving Ground, Tooele County, UT. An array of cargo containers, 2.5 m high \times 2.4 m wide \times 12.2 m long, was located nominally downwind of an unpaved road. The array consisted of 10 rows of cargo containers, spaced 6.4 m apart, with the long side oriented parallel to the road. Each row was 12 columns deep in the downwind direction with a space of 13.4 m between adjacent containers. This configuration resulted in a roughness height, z_0 , estimated from sonic anemometer data, of 0.71 m, corresponding approximately to a low-density residential area.

DustTraks and sonic anemometers were placed on towers located along the cargo array center line at 3 and 95 m downwind of the unpaved road. At the 3 m downwind tower, DustTraks were placed at 0.9, 1.7, and 3.7 m above grade and a 3-D sonic anemometer was located at 1.6 m above grade. At the 95 m tower, DustTraks were placed at heights of 1.8, 4.6, 9.1, and 18.3 m and 2-day sonic anemometers were placed at heights of 4, 8, 16, and 32 m. PM₁₀ dust was generated by driving a pickup truck back and forth on the unpaved road for a total of 44 trips. Tests were performed between 1:00 and 2:30 AM Mountain Daylight time on September 26, 2001. Analysis of sonic anemometry data gave a Monin–Obukhov length, L , of 310 m upwind of the container array and 1525 m in the center of the array, indicating that the atmosphere was well within the stable range in both cases. For the period of the experiment, winds were within 45° of the line perpendicular to the unpaved road.

Modeling Approach

A class of dispersion models that are known collectively as Gaussian plume models and that include the ISC3 short-term model⁸ is built on the approximation that a plume dispersing in the atmosphere assumes a shape similar to a normal distribution. These models work best for sources that are high above the ground, where dispersion in the vertical direction does not vary greatly with height. That is, the vertical dispersion can be assumed symmetrical about a horizontal plane located at the height of the source. The applicability and limitations of Gaussian approaches to dispersion modeling have been considered

by other investigators (e.g., Seinfeld and Pandis¹⁸), and an in-depth discussion is omitted here. Following the formulation described by the EPA,⁸ the basic equation for the ground-level concentration C ($\mu\text{g}/\text{m}^3$) downwind of a ground-level continuous line source of nonreactive material is:

$$C(z_r) = \sqrt{\frac{2}{\pi}} \frac{Q}{u_s \sigma_z} \exp\left[-0.5\left(\frac{z_r}{\sigma_z}\right)^2\right] \quad (10)$$

where Q is the line source emission rate (g/s/m), σ_z is the standard deviation of vertical concentration distribution, u_s is mean wind speed at the release height, z_r is a reference height, which is taken to be the larger of 1 m and $20 \times z_0$.⁸ The dispersion parameter σ_z is dependent on the downwind distance x and is given by the following equation:

$$\sigma_z = a(x_0 + x)^b \quad (11)$$

The parameters a and b , given by Turner,¹¹ are determined by the atmospheric stability and the distance downwind of the source.

When a vehicle passes over a road, the plume generated behind the vehicle has a discrete height in the vertical direction. This distance is a measure of the initial depth of the plume and is different from the plume release height. To account for the fact that the dust plume is initially dispersed by the turbulent wake of the vehicle, a “virtual” distance x_0 is added to the value of x in eq 11. The virtual distance x_0 is calculated by solving the equation for the initial value σ_{z0} . Because σ_z is the standard deviation of the concentration in the vertical direction assuming a normal distribution, then 95% of the plume is initially below the height $2 \times \sigma_{z0}$. Therefore, we may approximately define σ_{z0} as half the initial height of the plume generated by turbulence in the wake of a vehicle. A series of experiments performed during the same field campaign that has been described here were aimed at estimating the initial dust plume height behind a vehicle moving on an unpaved road.²⁸ Particle monitors and a sonic anemometer were mounted on a tower 3 m downwind of the road. Analysis of the plume height and the turbulent wake behind the vehicles indicated that for cars and small trucks, the initial plume was generally confined to less than 2 m above the ground. Based on these data, a value of 1 m was chosen to represent an approximation for σ_{z0} for all vehicles tested.

Dry deposition can be accounted for by numerically integrating the removal rate using the deposition velocity

(described in an earlier section) over the distance downwind of the source. If the removal by deposition is slow compared with the rate of dispersion, then it is a reasonable approximation to apply the fractional removal at each step to the entire concentration profile. In practice, this is only valid during neutral to unstable conditions and only when the deposition velocity is not too large. Other options are available for more accurate representation of the effect of deposition, and the ISC3 model accommodates their use. One such option allows for a modification to the Gaussian profile to address the fact that particles are removed at the ground and not uniformly from the entire vertical profile. In this work, no correction for the effect of deposition on the plume shape has been invoked.

This type of formulation for the dispersion and deposition of a pollutant is based on deposition to a horizontal surface from above that surface. It does not apply to flows where dispersion and deposition within the roughness elements are the dominant forms of transport (e.g., "impact zone" in Figure 1).

RESULTS AND DISCUSSION

In Figure 5 normalized concentrations at Towers 1, 2, and 3 are plotted on the same graph as the predicted Gaussian concentration profile. The PM_{10} concentration profile has a strong vertical gradient at Tower 1. This gradient decreases at Tower 2 and is even lesser further downwind at Tower 3. This indicates that although the dust plume is initially confined to a few meters above ground, it rapidly disperses as it is advected downwind. In general, the concentration gradients for the lower values of u_* are not as great as those at higher u_* values. This observation may invite the conclusion that lower values of u_* result in a greater degree of dispersion. It is important to note, however, that the transport time between the unpaved road and the towers is inversely proportional to u_* (see eq 8). Therefore, although smaller values of u_* appear to result in a greater degree of vertical dispersion compared with higher values of u_* at a given downwind distance, on a travel time basis the opposite is true. This effect can be seen by comparing the concentration profile at Tower 2 for $u_* = 0.2$ m/sec with that at Tower 3 for $u_* = 0.4$ m/sec, which represent comparable transport times.

The Gaussian plume model predictions are also plotted alongside the measurements in Figure 5. Because it was primarily formulated to describe dispersion of plumes aloft, the model does not allow for specification of a friction velocity. Rather, the value of σ_z is based solely on the atmospheric stability and the downwind distance. The stability during the Ft. Bliss experiments varied from neutral to very unstable, with slight to moderate instability being most prevalent. The measured concentration

profiles are in agreement with the model results for slightly to moderately unstable conditions. However, the model does not capture the differences in concentration gradient that are caused by variations in the friction velocity. For the conditions at Ft. Bliss where deposition appears to be minimal (see below), this may be a minor consideration but, in general, the inability of the model to account for variations in u_* may be a substantial shortcoming in other settings. For example, if the atmosphere is unstable but the average wind speed (and, consequently, u_*) is low, then the plume would be expected to spread quickly in the vertical direction even though it may not be advected substantially downwind. In this case, the Gaussian plume formulation would tend to overpredict particle removal as a function of downwind distance because it would assume higher near-ground concentrations than would actually exist. Similarly, if moderate winds exist under neutral or slightly stable conditions, then the model would underestimate the near-ground concentration as a function of downwind distance and would consequently underpredict deposition.

Normalized horizontal fluxes of PM_{10} measured at each of the three downwind towers during the 2002 Ft. Bliss experiments appear in Figure 6. For each pass, the horizontal flux measured at each tower was normalized by the flux calculated for Tower 1. Note that because of inherent natural variability, the results for individual passes differ substantially from one another. However, the aggregate average over 116 passes represented in Figure 6 has effectively filtered out the variability among individual passes. In addition, the vertical bars that represent standard errors of the mean normalized flux (i.e., standard deviation divided by the square root of the number of replicate measurements) in the figure are relatively small, allowing for quantitative comparison of the PM_{10} flux among the three towers. The normalized fluxes at Tower 1 and Tower 3 are, respectively, 1.000 ± 0.042 and 1.025 ± 0.043 . The difference between normalized fluxes at those two towers is 0.025 ± 0.060 , indicating that there is no statistically significant difference ($\alpha = 0.05$) between the horizontal fluxes measured at Towers 1 and 3. The lower limit of the 95% confidence interval for this difference is -0.095 ($0.025 - 2 \times 0.060$). That is, with the measurement method used, we are 95% confident that the difference between the fluxes at Tower 1 and 3 is less than 9.5%. Similar conclusions can be drawn when comparing normalized fluxes between Towers 1 and 2 and Towers 2 and 3. These findings are also qualitatively consistent with the preliminary results for the same field study presented by Etyemezian et al.²⁹ However, in that earlier work, only a subset of the data used to create Figure 6 were utilized.

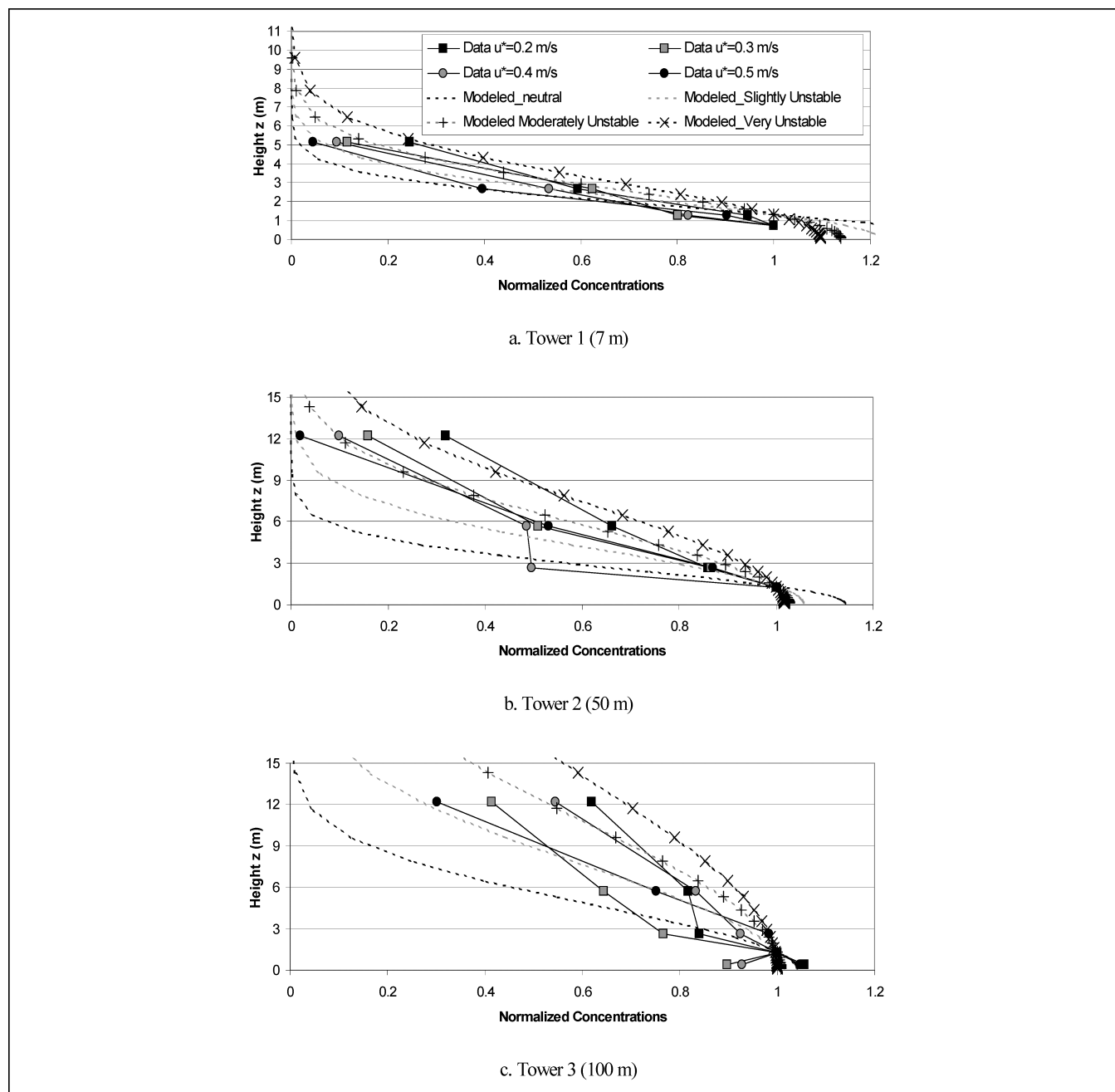


Figure 5. Concentration profiles normalized to measured and modeled concentration at 1.26 m above ground level at (a) Tower 1, 7 m downwind of unpaved road; (b) Tower 2, 50 m downwind; and (c) Tower 3, 100 m downwind. The y-axis in (a) differs from that in (b) and (c).

This point can be further supported by examining the particle size distributions measured at Towers 1 and 3. Figure 7 shows the ratio of particle concentrations measured at the same height (2.66 m) on both towers. The figure represents data from 137 individual passes where measured particle concentrations were significantly above background levels (i.e., greater than background concentration plus three standard deviations) at both Tower 1 and Tower 3. Note that in the earlier work of Etyemezian et al.²⁹ this criterion was not in place, and the data in the corresponding figure are slightly different from those shown in the present paper. The x-axis shows the

estimated mean geometric diameter for the size bin measured (see eqs 5 and 6).

Because the smallest size bin shown, represented by particles with diameters of 3.9 μm , is not expected to deposit to any appreciable extent, concentrations of all other size bins were normalized by that of 3.9- μm particles. Thus, the y-axis in the figure corresponds to the fraction of particles in the stated size bin that remains in suspension 100 m downwind of the unpaved road. In general, the removal rate of particles increases with diameter; this is consistent with the expectation that the deposition velocity v_d also increases with diameter. Figure 7

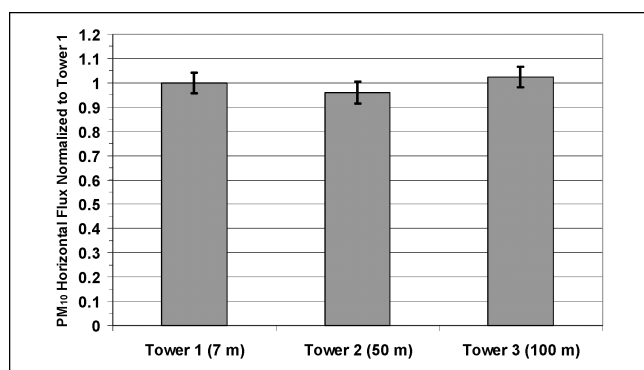


Figure 6. Comparison of horizontal flux at the three downwind towers. Data are averaged over 116 individual passes when the wind direction was within 45° of perpendicular to the road and all three towers were functioning. Fluxes were calculated according to eq 7 and normalized to values at Tower 1. Vertical bars represent standard errors.

also shows the model prediction of the size-dependent particle removal rates. The average friction velocity ($u_* = 0.35$ m/sec) over the 137 individual passes was used in evaluating the modeled particle deposition velocities. At a downwind distance of 100 m, the removal of particles with aerodynamic diameter of 9.9 μm or less is not measurable. Note that this also corroborates that a difference in PM₁₀ flux between Tower 1 and Tower 3 would not be measurable with the DustTrak instruments used. According to the model results, only 4.3% of 9.9- μm particles are removed by the time the dust plume has traveled 100 m. Larger particle sizes with higher deposition velocities are

measurably removed at those same distances. For example, the removal of 19.7- μm particles between Tower 1 and Tower 3 is 25% ($\pm 17\%$) according to the measurements and 11% based on model results. Measurements of removal of large particles (9.9 μm and larger) between Tower 1 and Tower 3 with the GRIMM optical particle counters are subject to substantial uncertainty because the number concentrations of large particles are comparatively low and those measurements are therefore less statistically robust than for smaller, more abundant particles.

In contrast to the field experiment described here, the work performed by Veranth et al.³ examined the removal of PM₁₀ unpaved road dust over a distance of 95 m under nighttime stable atmospheric conditions and over terrain that approximates a low-density residential area in terms of surface roughness. Thus, whereas conditions at Ft. Bliss (small surface roughness and unstable atmosphere) serve to minimize particle deposition in the vicinity of a ground-based dust source, the experiment by Veranth et al.³ represents the opposite extreme. Stable conditions serve to keep the dust plume close to the ground, allowing particles a greater opportunity for deposition by gravity settling and by impaction upon the surface roughness elements.

To calculate the horizontal flux of PM₁₀ at both the 3- and 95-m downwind towers, Veranth et al.³ used fitting functions for both the vertical wind profile, $u(z,t)$, and the

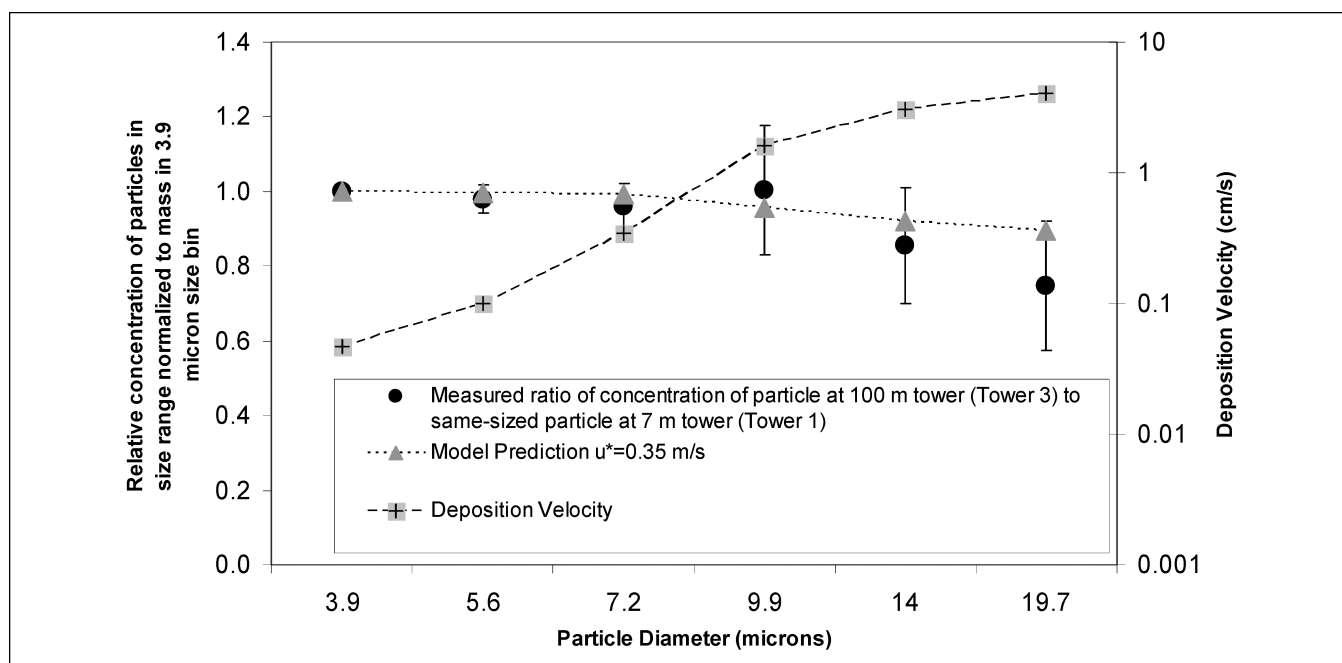


Figure 7. Comparison of particle size distributions at Towers 1 and 3 measured by GRIMM 1.108 OPC with model predictions. Data are averaged over the 137 individual passes where data were available from both Tower 1 and Tower 3. The x-axis shows particle aerodynamic diameter calculated by assuming a density of 2.6 g/cm³ and geometric mean diameter representing each size bin. Particle concentrations at Towers 1 and 3 were each normalized by concentration of 3.9- μm particles. The left y-axis represents ratios of normalized concentrations. The right y-axis corresponds to the deposition velocity used in the case of each particle size.

concentration profile, $C(z, t)$, and integrated the product to obtain the flux according to

$$F_x = \int_{z=0}^{z=\infty} \int_{t=0}^{t=t_{\max}} C_x(z, t) \cdot u_x(z, t) \cdot dt dz \quad (12)$$

where t_{\max} is the duration of passing of the dust plume by the tower and the subscript x indicates the location of the tower. Both a power law and exponential form were considered for the vertical wind profile. Power law, Gaussian distribution, and exponential profiles were considered for the dust concentration profile. Veranth et al.³ reported that, depending on the choices for wind and concentration profile fitting functions, between 86% and 89% of the PM_{10} was removed by deposition within the first 95 m of transport downwind of the road. If we assume a plume height of 2 m in the immediate wake of a passing vehicle (as was done for the Ft. Bliss study), then the dust plume would initially be submerged within the 2.5-m high cargo containers used as roughness elements. Veranth et al.³ calculated the differential dust flux versus height, and their results indicated that at 95 m approximately half the dust flux was still below the 2.5-m container height, suggesting that the entire experiment domain involved the “impact zone” (see Figure 1).

In contrast, the Gaussian model, assuming very stable atmospheric conditions and the roughness length ($z_0 = 0.71$ m) estimated by Veranth et al.,³ predicts that only 30% of the PM_{10} would have deposited over the same distance. This large discrepancy between model results and measured values can be attributed, in part, to the fact that the model assumes that the surface roughness is small compared with the height of the plume at the junction of the road and the downwind terrain. This assumption may be violated in the comparatively complex geometry of the cargo containers under stable conditions, where one would expect that much of the transport would occur by channeling between containers. That is, the model is applicable in the “near source” region, and the first 95 m of downwind transport in a cargo container setting may still correspond to the “impact region” (see Figure 1). Related to this, the assumption of a Gaussian concentration profile near the ground requires that the wind speed not change substantially with height. In the case of the flat terrain of Ft. Bliss, this assumption holds better than in the case of the cargo containers, which act as a significant momentum sink, thereby influencing the vertical wind profile to a greater degree.

The daytime atmospheric stability and sparse vegetation conditions of the Ft. Bliss field study are applicable to unpaved roads in rural areas of the southwest United States. PM dust deposition from unpaved road emissions

may be higher in situations with different atmospheric stability and surface roughness conditions, such as arid regions in winter, unpaved roads in agricultural settings (greater roughness lengths), and urban perimeter settlements in developing countries.

CONCLUSIONS

For the purposes of modeling the transport and removal of dust particles near an unpaved road source, Gaussian-style models, such as the EPA’s ISC3, appear to provide a simplistic but reasonable preliminary approach. Dispersion and deposition are the two main processes that must be accounted for in any model used. The Gaussian models use distance-based dispersion parameters that depend on atmospheric stability (σ). Comparison of predicted concentration profiles with those observed at Ft. Bliss indicated that the models captured the approximate shape of the dust plume. However, whereas the measured profiles varied in vertical concentration gradient at different values of the friction velocity u_* , the Gaussian-predicted profile was invariant. This is because the friction velocity is not included in the parameterization of σ .

Though the similarity between the concentration profiles measured at Ft. Bliss and those predicted by the Gaussian plume model is encouraging, it is difficult to determine how well models for deposition velocity reflect real-world values. This is largely because these models have not been widely tested with field data. In many cases,^{4,15} adjustable parameters are made to fit wind tunnel tests for deposition on a limited variety of surfaces. The applicability of these models under varying land use and atmospheric conditions is not well known.

Comparison of model results with measurements conducted under conditions of urban-scale roughness and stable atmospheric stratification³ indicates that the model may substantially underpredict the removal of PM_{10} in that type of setting. The modeling effort reported here only accounts for the deposition of particles in the “near-source” region, and it is likely that the conditions of the Veranth et al.³ experiment more closely resembled the “impact zone.” It is clear that some modifications should be implemented to improve the model’s performance for the type of setting described by Veranth et al.³ At present, there is a shortage of field measurements and a thorough test of the model is not possible. Future research efforts should be directed at obtaining measurements under varying conditions of land use (surface roughness) and atmospheric stability.

ACKNOWLEDGMENTS

The authors thank Bob Lebens (WESTAR), Duane Ono (Great Basin Unified APCD), Mark Scruggs (National Park Service), Pat Arnott, Judith Chow, Mark Green, Hans

Moosmuller, Ravi Varma, John Walker (Desert Research Institute), Marc Pitchford (NOAA), Geary Schwemmer and Dave Miller (NASA), Raed Laban, Gauri Seshadri (University of Utah), Clyde Durham (Ft. Bliss), and Thompson Pace (EPA) for contributing to the completion of this work through equipment loans, comments on the manuscript, and assistance in data analysis. This work was funded by the WESTAR Council and DoD SERDP Grants CP1190 and CP1191. Field testing was made possible through the cooperation of the United States Army at Ft. Bliss.

REFERENCES

1. Watson, J.G.; Chow, J. *Reconciling Urban Fugitive Dust Emissions Inventory and Ambient Source Contribution Estimates: Summary of Current Knowledge and Needed Research*. DRI Document No. 6110.4F; U.S. Environmental Protection Agency, Desert Research Institute: Reno, NV, 2000.
2. Countess, R. *Methodology for Estimating Fugitive Windblown and Mechanically Resuspended Road Dust Emissions Applicable for Regional Scale Air Quality Modeling*; Western Governors Association by Countess Environmental: Westlake Village, CA, 2001.
3. Veranth, J.M.; Seshadri, G.; Pardyjak, E. Vehicle-Generated Fugitive Dust Transport: Analytic Models and Field Study; *Atmos. Environ.* **2003**, *37*, 2295–2303.
4. Raupach, M.R.; Wood, N.; Dorr, G.; Leys, J.F.; Cleugh, H.A. The En-trapment of Particles by Windbreaks; *Atmos. Environ.* **2001**, *35*, 3373–3383.
5. Lamb, R.G.; Duran, D.R. Eddy Diffusivities Derived from a Numerical Model of the Convective Boundary Layer; *Nuovo. Cimento.* **1977**, *1c*, 1–17.
6. Shir, C.C. A preliminary Numerical Study of Atmospheric Turbulent Flows in the Idealized Planetary Boundary Layer; *J. Atmos. Sci.* **1973**, *30*, 1327–1339.
7. Venkatram, A. The Parametrization of the Vertical Dispersion of A Scalar in the Atmospheric Boundary Layer; *Atmos. Env.* **1993**, *27A*, 1963–1966.
8. U.S. EPA. *User's Guide for the Industrial Source Complex (ISC3) Dispersion Models Volume II: Description of Model Algorithms*; U.S. Environmental Protection Agency, Office of Air Quality Planning and Standards: Emissions, Monitoring, and Analysis Division: Research Triangle Park, NC, 1995.
9. Gifford, F.A. Use of Routine Meteorological Observations for Estim-ating Atmospheric Dispersion; *Nucl. Safety* **1961**, *2*, 47–51.
10. Klug, W. A Method for Determining Diffusion Conditions for Synop-tic Observations; *Staub. Reinhalt. Luft.* **1969**, *29*, 14–20.
11. Turner, D.B. *Workbook of Atmospheric Dispersion Estimates. PHS Publi-cation No 999-AP-26*; U.S. Department of Health, Education and Wel-fare, National Air Pollution Control Administration: Cincinnati, OH, 1970.
12. Martin, D.O.; Comment on the Change of Concentration Standard Deviations with Distance; *J. Air Pollut. Control Assoc.* **1976**, *26*, 145–146.
13. Du, S.; Venkatram, A. A Parametrization of Vertical Dispersion of Ground-Level Releases; *J. Appl. Meteorol.* **1997**, *36*, 1004–1015.
14. Schopflocher, T.P.; Sullivan, P.J. A Mixture Model for the PDF of a Diffusing Scalar in a Turbulent Flow; *Atmos. Environ.* **2002**, *36*, 4405–4417.
15. Slinn, W.G.N. Predictions for Particle Depositions to Vegetative Can-opies; *Atmos. Environ.* **1982**, *16*, 1785–1794.
16. Wu, Y.L.; Davidson, C.I.; Dolske, D.A.; Sherwood, S.I. Dry Deposition of Atmospheric Contaminants: The Relative Importance of Aerody-namic, Boundary Layer, and Surface Resistances; *Aerosol Sci. & Technol.* **1992a**, *16*, 65–81.
17. Etymezian, V.; Davidson, C.I.; Finger, S.; Striegel, M.; Barabas, N.; Chow, J. Vertical Gradients of Pollutant Concentrations and Deposi-tion Fluxes on a Tall Limestone Building; *J. Am. Inst. Conservat.* **1997**, *37*, 187–210.
18. Seinfeld, J.H.; Pandis, S.N. *Atmospheric Chemistry and Physics: From Air Pollution to Climate Change*. Wiley Interscience: New York, 1997.
19. Willeke, K.; Xu, M. Impaction and Rebound of Particles from Surfaces. *J. Aerosol Sci.* **1992**, *23 (Suppl.)*, S15–S18.
20. Wu, Y.L.; Davidson, C.I.; Lindberg, S.E.; Russell, A.G. Resuspension of Particulate Chemical Species at Forested Sites; *Environ. Sci. & Technol.* **1992b**, *26*, 2428–2435.
21. Byun, D.W.; Dennis, R. Design Artifacts in Eulerian Air Quality Mod-els: Evaluation of the Effects of Layer Thickness and Vertical Profile Correction on Surface Ozone Concentrations; *Atmos. Environ.* **1995**, *29*, 105–126.
22. Pleim, J.; Venkatram, A.; Yamartino, R. *ADOM/TADAP Model Develop-ment Program, Volume 4. The Dry Deposition Module*. Ontario Ministry of the Environment: Rexdale, Ontario, 1984.
23. Gillies, J.A.; Watson, J.G.; Rogers, C.F.; Dubois, D.; Chow, J.C.; Lang-ston, R.; Sweet, J. Long-term efficiencies of dust suppressants to re-duce PM₁₀ emissions from unpaved roads; *J. Air & Waste Manage. Assoc.* **1999**, *49*, 3–16.
24. Cowherd, C. *Profiling Data for Open Fugitive Dust Sources*; Prepared for U. S. Environmental Protection Agency, Emissions Factor and Inven-tory Group, Office of Air Quality Planning and Standards, RTP, NC, by Midwest Research Institute: Kansas City, MO, 1999.
25. Niu, J.; Lu, B.M.K.; Tung, T.C.W. Instrumentation Issue in Indoor Air Quality Measurements: The Case with Respirable Suspended Particu-lates; *Indoor Built Environ.* **2002**, *11*, 162–170.
26. Moosmüller, H.; Arnott, W.P.; Rogers, C.F.; Bowen, J.L.; Gillies, J.A.; Pierson, W.R.; Collins, J.F.; Durbin, T.D.; Norbeck, J.M. Time Resolved Characterization of Diesel Particulate Emissions. 1. Instruments for Particle Mass Measurement; *Environ. Sci. Technol.* **2001**, *35*, 781–787.
27. Chung, A.; Chang, D.P.Y.; Kleeman, M.J.; Perry, K.D.; Cahill, T.A.; Dutcher, D.; McDougall, E.M.; Stroud, K. Comparison of Real-Time Instruments Used to Monitor Airborne Particulate Matter; *J. Air & Waste Manage. Assoc.* **2001**, *51*, 109–120.
28. Etymezian, V.; Gillies, J.; Kuhns, H.; Nikolic, D.; Watson, J.; Veranth, J.; Labban, R.; Seshadri, G.; Gillett, D. *Field Testing and Evaluation of Dust Deposition and Removal Mechanisms: Final Report*; Report Prepared for WESTAR Council, Lake Oswego, OR, by DRI: Las Vegas, NV, 2003.
29. Etymezian, V.; Gillette, D.; Gillies, J.; Kuhns, H.; Nikolic, D.; Veranth, J.; Watson, J. PM₁₀ Emissions Factors for Unpaved Roads: Correction for Near-Field Deposition; *PM AAAR 2003: Atmospheric Sciences, Expo-sure, Health and Welfare Effects, Policy*. Presented at the American Association for Aerosol Research, Pittsburgh, PA, March 31 through April 4, 2003.

About the Authors

Vic Etymezian is associate research professor at the Desert Research Institute (DRI) in Las Vegas, NV. John Gillies and Hampden Kuhns are associate research profes-sors in the Division of Atmospheric Sciences at the DRI in Reno, NV. Dale Gillette is a physical scientist at Air Re-sources Laboratory, NOAA, in Research Triangle Park, NC. Sean Ahonen and Djordje Nikolic are research affiliates at DRI in Las Vegas, NV. John Veranth is a research assistant professor at the Department of Pharmacology and Toxicol-ogy at the University of Utah, Salt Lake City, UT. Address correspondence to: Vic Etymezian, Division of Atmo-spheric Sciences, DRI, 755 E. Flamingo Rd., Las Vegas, NV 89119; phone: (702) 895-0569; e-mail: vic@dri.edu.